

VarMixup: Exploiting the Latent Space for Robust Training and Inference

Puneet Mangla, Vedant Singh, Shreyas Jayant Havaladar, and Vineeth N Balasubramanian

IIT Hyderabad, India

{cs17btech11029,cs18btech11047,cs18btech11042,vineethnb}@iith.ac.in

Abstract. The vulnerability of Deep Neural Networks (DNNs) to adversarial attacks has led to development of many defense approaches. Among them, Adversarial Training (AT) is a popular and widely used approach for training adversarially robust models. Mixup Training (MT), a recent popular training algorithm, improves generalization performance of models by introducing globally linear behavior in between training examples. Although still in its early phase, we observe a shift in trend of exploiting Mixup from perspectives of generalisation to that of adversarial robustness. It has been shown that the Mixup trained models improves robustness of models but only passively. A recent approach, Mixup Inference (MI), proposes an inference principle for Mixup trained models to counter adversarial examples at inference time by mixing the input with other random clean samples. In this work, we propose a new approach - *VarMixup* (*Variational Mixup*) - to better sample mixup images by using the latent manifold underlying the data. Our experiments on CIFAR-10, CIFAR-100, SVHN and Tiny-Imagenet demonstrate that *VarMixup* beats state-of-the-art AT techniques without training the model adversarially. Additionally, we also conduct ablations that show that models trained on *VarMixup* samples are also robust to various input corruptions/perturbations, have low calibration error and are transferable.

Keywords: Adversarial Robustness, Mixup, Mixup Inference

1 Introduction

Deep Neural Networks (DNNs) have become a key ingredient to solve many challenging tasks like classification, segmentation, object detection, speech recognition, etc. However, it is now known that they can be fooled by applying imperceptible perturbations, called adversarial perturbations, to input examples leading to wrong predictions[41,14]. Over the past few years, various approaches [47,21,1,8,27,14,49,30,29] have been proposed to craft adversarial examples by maximizing the network's prediction error in distinct ways. As a consequence, it has become quite risky to deploy them in safety-critical applications including autonomous navigation or healthcare. Efforts [27,14,36,38,55,35,31,12,44] have been made in recent years to make models robust to these adversarial perturbations. Among the proposed methods, Adversarial Training (AT) [38,27,14,56,25]

has emerged as a popular and widely used algorithm to obtain adversarially robust models. Several variants of adversarial training have been proposed lately with motivation of inducing *local linearity* [35] by training networks using adversarial examples. However, training robust models using AT is not only computationally expensive but suffers from a performance degradation on clean examples [43]. Though some recent attempts [37,53] have managed to adversarially train models in a low computational budget, they still suffer from the trade-off between standard accuracy and robustness to adversarial perturbations.

On the other hand, Mixup Training (MT) [57] has emerged as a popular technique to train models having both better generalisation and robustness. However, robustness performance of Mixup trained models is significantly lower than AT techniques [25,27] when it comes to strong adversarial attacks like PGD [27], structural [49] or functional attacks. Taking advantage of the *induced global linearity* in between training examples by MT, Pang et al. [33] proposed Mixup Inference (MI) to exploit this global linearity at inference time and better defend Mixup-trained models against adversarial attacks. Though MI has been shown to significantly boost adversarial robustness of Mixup-trained models, the performance outperforms AT only when applied on top of Interpolated Adversarial Training [25], which is yet another adversarial training technique.

Although still in its early phase, the above efforts [57,46,33] indicate a trend to viewing Mixup from a robustness perspective.

In this work, we take another step in this direction and propose a sampling technique called *VarMixup* (*Variational Mixup*) to sample better Mixup images during training and inference to induce adversarial robustness. In particular, we hypothesize that the latent unfolded manifold underlying the data (through a generative model, a Variational Autoencoder in our case) is linear by construction, and hence more suitable for the linear interpolations used in Mixup. Importantly, we show that this choice of the distribution for Mixup plays an important role towards adversarial robustness (Section 3). Our experiments on 4 standard datasets- CIFAR-10, CIFAR-100, SVHN,

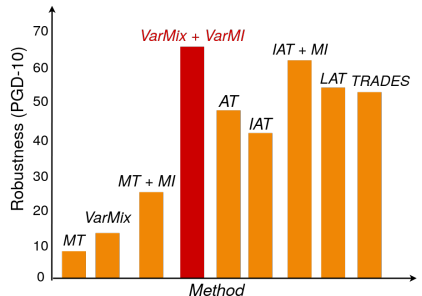


Fig. 1: Performance of Mixup Training (MT) [57], Mixup-Inference (MI) [33], Adversarial training (AT) [27], TRADES [56], LAT [38], IAT [25] and VarMixup (ours)

Tiny-Imagenet shows that VarMixup when combined with Mixup training and inference, beats state-of-the-art adversarial training techniques (like PGD [27] and IAT [25]) under oblivious attacks without training model adversarially. We conduct several other studies to examine the proposed method, and obtain promising results across all these experiments.

Our contributions can be summarized as follows:

- We propose a new sampling technique, VarMixup, which when combined with Mixup training and inference, outperforms adversarial training (by 5-

10%) techniques without training the model in adversarial fashion. To the best of our knowledge, this is the first sampling technique explicitly proposed for adversarial robustness, and also the first among Mixup methods to consider the latent unfolded manifold for interpolation.

- Additionally, we show that models trained using VarMixup samples are robust to common corruptions and perturbations, have low calibration error and are transferable.
- We also conduct a comprehensive set of studies which show that VarMixup significantly decreases the local linearity error of the neural network and generates samples that are slightly off-distribution from training examples or mixup generated samples, to provide robustness.

2 Related Work

We briefly discuss earlier efforts in adversarial attacks and defenses, as well as Mixup-based methods, that are closest to this work.

Adversarial Attacks and Defenses Adversarial Attacks can be mainly classified into three categories: White-box attacks [30,27,47,14], Black-box attacks [21,1,34,8] and Oblivious attacks [9]. In the white-box setting, the adversary has full access to the network; and in the black-box setting, the adversary has no information about the network. Oblivious adversaries are not aware of the existence of the defense mechanism, and generate adversarial examples based on the unsecured classification model. With this advancement in adversarial attacks every year, various defenses have been proposed to counter them. Parseval networks [12] and Lipplitchz Margin Training [44] train robust models by reducing their Lipschitz constant. LAT [38], Feature denoising [48], and Feature Scattering [55] achieve robustness by harnessing the fact that latent layers can help defend to perturbations. TRADES [56] presents a new defense method that provides a trade-off between adversarial robustness and accuracy by decomposing the prediction error for adversarial examples (robust error) as the sum of the natural (classification) error and boundary error. Among the proposed approaches, Adversarial Training (AT) [27,14,25,28] is a popular and widely opted strategy. The objective of AT is to train models on adversarial examples at every step of training to better match the adversarial distribution encountered at test time. Qin et al. [35] show that AT techniques make the loss landscapes of networks locally linear, and propose a regularizer that encourages the loss to behave linearly in the vicinity of the training data. A similar work [31] acts as a network regularizer by directly minimizing curvature of their loss surface, leading to adversarial robustness that is on par with adversarial training. Though AT is an effective way of improving the robustness of deep networks, they are usually computationally expensive. To address this drawback of AT, recent approaches [37,54] aim to reduce adversarial training overhead by recycling gradients and accelerating via the maximal principle respectively. For a comprehensive review of the work done in the area of adversarial examples, please refer [51].

Mixup: Mixup [57] is a recent method that trains networks on convex combinations of data pairs and their labels. By doing so, it regularizes the network

to behave linearly in between training examples, thus inducing global linearity between them. A recent variant, Manifold Mixup [46], exploits interpolations at hidden representations, thereby obtaining neural networks with smoother decision boundaries at different levels of hidden representations. AugMix [19] mixes up multiple augmented images and uses a Jensen-Shannon Divergence consistency loss on them to achieve better robustness to common input corruptions [18]. In semi-supervised learning, MixMatch [4] obtains state-of-the-art results by guessing low-entropy labels for data-augmented unlabeled examples and mixes labeled and unlabeled data using Mixup. It has been shown that apart from better generalization, Mixup also improves the robustness of models to adversarial perturbations but not as significantly as AT. To further boost this robustness at inference time, Pang et al. [33] recently proposed a Mixup Inference technique which performs a mixup of input x with a clean sample x_s and passes the corresponding mixup sample $(\lambda \cdot x + (1 - \lambda) \cdot x_s)$ into the classifier as the processed input. Their analysis indicates that MI imposes a tighter upper bound on the potential attack ability for a crafted perturbation leading to robustness to adversarial attacks. Other efforts on Mixup [42] have shown that Mixup-trained networks are significantly better calibrated than ones trained in the regular fashion. These recent efforts have shown the potential of Mixup-based methods, which we exploit in the latent space for state-of-the-art robustness results.

Comparison with Other Mixup-related Work: Considering the recent popularity of Mixup-based methods, we address how our work is different from other recent efforts in Mixup. Xu et al. [50] use domain mixup to improve the generalization ability of models in domain adaptation. Adversarial Mixup Resynthesis [3] involves mixing latent codes used by autoencoders through an arbitrary mixing mechanism that can recombine codes from different inputs to produce novel examples. This work however has a different objective and focuses on generative models in a GAN-like setting, while our work focuses on adversarial robustness, which is a different objective. The work by Liu et al. [26] might be closest to ours in terms of approach as they introduce the adversarial autoencoder (AAE) to impose the feature representations with uniform distribution and apply the linear interpolation on latent space. However, their work deals from a generalization perspective, and results show marginal improvements. In our work, we directly exploit the manifold learned by VAE (and do not regularize it unlike the previous work) for the mixup and report improved adversarial robustness. Moreover, we also present useful insights into the working of VarMixup (leading to robustness), which is lacking in earlier work including [26], thus making our contributions different and more complete.

3 Methodology

3.1 Notations and Preliminaries

We denote a neural network as $F_w : \mathbb{R}^{c \times h \times w} \rightarrow \mathbb{R}^k$, with weight parameters w .

F_w takes an image $x \in \mathbb{R}^{c \times h \times w}$ and outputs logits, $F_w^i(x)$ for each class $i \in \{1 \dots k\}$. Without loss of generality, we assume the classification task, and \mathcal{L} denotes the standard cross-entropy loss function. p_{actual} denotes the training data distribution, and the optimal weight parameter, w^* , obtained by training the network using standard empirical risk minimization

is given by: $w^* = \arg \min_w \mathbb{E}_{(\mathbf{x}, y) \sim p_{\text{actual}}} [\mathcal{L}(F_w(\mathbf{x}), y)]$. Here y is the true label associated with input x . We now briefly introduce the concepts relevant to this work, before describing our methodology.

Adversarial Attacks: In this work, we consider L_∞ bounded *Projected Gradient Descent Attack (PGD)* [27] which is a more powerful, multi-step variant of *FGSM* [14] attack, and commonly considered among the state-of-the-art adversarial attacks. The adversary of input x is computed as follows:

$$\mathbf{x}^0 = \mathbf{x}; \mathbf{x}^{t+1} = \Pi_{\mathbf{x}+S}(\mathbf{x}^t + \alpha \text{sign}(\nabla_{\mathbf{x}} \mathcal{L}(F_w(\mathbf{x}), y))) \quad (1)$$

where α is the step size, Π is the projection function, and S is the space of possible perturbations. For more details, we refer the interested reader to [27].

Adversarial Training (AT): This is used to train the model in a robust manner by continuously augmenting the data with adversarial perturbations, to match the training distribution with the adversarial test distribution [14,27]. Essentially, for AT, the optimal parameter w^* is given by:

$$w^* = \arg \min_w \mathbb{E}_{(\mathbf{x}, y) \sim p_{\text{actual}}} \left[\max_{\delta \in S} \mathcal{L}(F_w(\mathbf{x} + \delta), y) \right] \quad (2)$$

Here, the inner maximization $\max_{\delta \in S} \mathcal{L}(F_w(\mathbf{x} + \delta), y)$ is calculated using a strong adversarial attack such as PGD.

Mixup: [57] proposed a method to train models on the convex combination of pairs of examples and their labels. In other words, it constructs virtual training examples as: $x' = \lambda \cdot x_i + (1 - \lambda) \cdot x_j$; $y' = \lambda \cdot y_i + (1 - \lambda) \cdot y_j$, where x_i, x_j are input vectors; y_i, y_j are one-hot label encodings and λ is a mixup coefficient, usually sampled from a $\beta(\eta, \eta)$ distribution. Its variant, *Manifold Mixup* [46], a more recent method, trains neural networks on linear combinations of hidden

Mixup performs linear interpolations on the data space, assuming an induced global linearity on this space.

VarMixup performs linear interpolations on the unfolded latent manifold, which by construction is expected to be linear, thereby supporting more effective linear interpolations in this space.

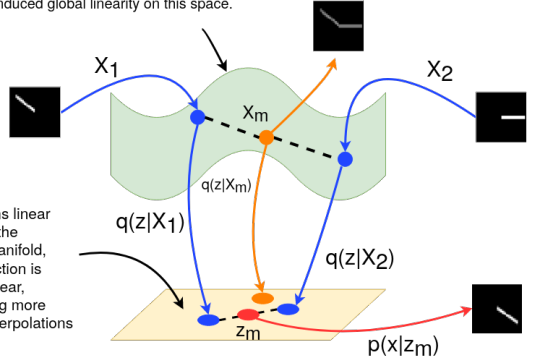


Fig. 2: Illustration of conceptual idea behind VarMixup. We interpolate on the unfolded manifold, as defined by a generative model (VAE, in our case).

representations of training examples.

Mixup Inference: [33], a recently developed specialized inference principle for mixup-trained models, attempts to break the locality of adversarial perturbations. Assuming that F_w is a pre-trained mixup model, the output scores using MI, $F_w^{MI}(x)$, on an input x is given by:

$$F_w^{MI}(x) = \mathbb{E}_{x_s \sim p_{MI}} F_w(\lambda_{MI} \cdot x + (1 - \lambda_{MI}) \cdot x_s) \quad (3)$$

Here, $\lambda_{MI} \in [0, 1]$ is a fixed mixup coefficient and p_{MI} is known as a sampling pool which differs for different variants of MI. In this work, we consider MI-OL (MI with other labels), where the sampling pool p_{MI} contains examples uniformly belonging to all classes except the predicted class of x . The expectation can be approximated by averaging over N_{MI} runs.

3.2 Background: Vicinal Risk Minimization

Given the data distribution p_{actual} , a neural network F_w and loss function \mathcal{L} , the *expected risk* (average of loss function over p_{actual}) is given by $R(F_w) = \int \mathcal{L}(F_w(x), y) \cdot dp_{actual}(x, y)$. In practice, the true distribution p_{actual} is unknown, and is approximated by the training dataset $D = \{(x_i, y_i)\}_{i=1}^N$, which represents the *empirical distribution*: $p_\delta(x, y) = \frac{1}{N} \cdot \sum_{i=1}^N \delta(x = x_i, y = y_i)$. Here, $\delta(x = x_i, y = y_i)$ is the Dirac delta function centered at (x_i, y_i) . Using p_δ as an estimate to p_{actual} , we define *expected empirical risk* as:

$$R_\delta(F_w) = \frac{1}{N} \cdot \sum_{i=1}^N \mathcal{L}(F_w(x_i), y_i) \quad (4)$$

Minimizing Eqn 4 to find optimal F_w^* is typically termed *Empirical Risk Minimization (ERM)*. However overparametrized neural networks can suffer from memorizing, leading to undesirable behavior of network outside the training distribution, p_δ . Addressing this concern, Chapelle et al. proposed *Vicinal Risk Minimization (VRM)*, where p_{actual} is approximated by a vicinal distribution p_v , given by:

$$p_v(x, y) = \frac{1}{N} \cdot \sum_{i=1}^N v(x, y | x_i, y_i) \quad (5)$$

where v is the *vicinal distribution* that calculates the probability of a data point (x, y) in the vicinity of other samples (x_i, y_i) . Thus, using p_v to approximate p_{actual} , *expected vicinal risk* is given by:

$$R_v(F_w) = \frac{1}{N} \cdot \sum_{i=1}^N g(F_w, \mathcal{L}, x_i, y_i) \quad (6)$$

where $g(F_w, \mathcal{L}, x_i, y_i) = \int \mathcal{L}(F_w(x), y) \cdot dv(x, y | x_i, y_i)$. Popular examples of vicinal distributions include: (i) *Gaussian Vicinal distribution*: Here, $v_{gaussian}(x, y | x_i, y_i) = \mathcal{N}(x - x_i, \sigma^2) \cdot \delta(y = y_i)$, which is equivalent to augmenting the training samples with Gaussian noise; and (ii) *Mixup Vicinal distribution*: Here $v_{mixup}(x, y | x_i, y_i) = \frac{1}{n} \cdot \sum_{j=1}^N \mathbb{E}_\lambda[\delta(x = \lambda \cdot x_i + (1 - \lambda) \cdot x_j, y = \lambda \cdot y_i + (1 - \lambda) \cdot y_j)]$, where $\lambda \sim \beta(\eta, \eta)$ and $\eta > 0$.

From a perspective of adversarial robustness, analogous to previous definitions, we define *adversarial risk* in this work as:

$$\begin{aligned}
 R^{adv}(F_w) &= \int \max_{\delta \in S} \mathcal{L}(F_w(x + \delta), y) \cdot dp_{actual}(x, y) \\
 R_{\delta}^{adv}(F_w) &= \frac{1}{N} \cdot \sum_{i=1}^N \max_{\delta \in S} \mathcal{L}(F_w(x_i + \delta), y_i) \\
 R_v^{adv}(F_w) &= \frac{1}{N} \cdot \sum_{i=1}^N \max_{\delta \in S} g(F_w, \mathcal{L}, x_i + \delta, y_i)
 \end{aligned} \tag{7}$$

where S is the space of allowed perturbations.

Let $F_{w^*}^v$ be the solution of minimization of vicinal adversarial risk, $R_v^{adv}(F_w)$. Then, following (cf. Eqn 11 in) [52], the quantity $R^{adv}(F_{w^*}^v) - R_v^{adv}(F_{w^*}^v)$ corresponds to the estimation of the expected adversarial risk of $F_{w^*}^v$ from its vicinal adversarial risk, and this can be bounded as:

$$R^{adv}(F_{w^*}^v) - R_v^{adv}(F_{w^*}^v) \leq \sup_{F_w} \{R^{adv}(F_w) - R_v^{adv}(F_w)\} \tag{8}$$

which we call the robustness bound for VRM. Note again that this bound is analogous to the generalization bound for VRM in [52]. Motivated by this bound, we propose an approach to leverage the vicinal distribution to achieve adversarial robustness. From Eqn 8, we observe that the bound depends on two factors: (1) the choice of vicinal distribution v and (2) the choice of family neural networks F_w . In this work, we limit the choice of F_w to ResNets [17] (specifically ResNet-34), thereby restricting the function class, and study the choice of vicinal distribution. Considering the recent success of using Mixup as a vicinal distribution for generalization [57] and Mixup inference for state-of-the-art adversarial robustness [33], we choose to consider a vicinal distribution based on Mixup-based linear interpolations. However, we propose the use of vicinal distributions from latent spaces in this work. We explain this choice below.

The use of generative models such as Variational Autoencoders (VAEs) [23] to capture the latent space from which a distribution is generated provides us an unfolded manifold (the low-dimensional latent space), where the linearity in between training examples is more readily observed. Defining vicinal distributions by using neighbours on this latent manifold (which is linear in the low-dimensional space) learned by generative models hence provides us more effective linear interpolations than the ones in input space. We use a generative model to capture the induced global linearity in between examples on a latent manifold, and define mixup vicinal distributions on this latent surface.

3.3 Our Approach: VarMixup (Variational Mixup)

To capture the latent manifold of the training data through a generative model, we opt for a Variational Autoencoder (VAE). VAE [23] is an autoencoder which is trained using Variational Inference, which serves as an implicit regularizer to ensure that the obtained latent space allows us to generate new data from the same distribution as training data.

We denote the encoding and decoding distribution of VAE as $q_\phi(z|x)$ and $p_\theta(x|z)$ respectively, parameterized by ϕ and θ respectively. Given $p(z)$ as the desired prior distribution for encoding, the general VAE objective is given by the loss function:

$$\mathcal{L}_{VAE} = -\gamma \cdot D(q_\phi(z)||p(z)) + \mathbb{E}_{x \sim p_{actual}} \mathbb{E}_{z \sim q_\phi(z|x)} [\log(p_\theta(x|z))] \quad (9)$$

Here, D is any strict divergence, meaning that $D(q||p) \geq 0$ and $D(q||p) = 0$ if and only if $q = p$, and $\gamma > 0$ is a scaling coefficient. The second term in the objective act as a image reconstruction loss and $q_\phi(z) = \mathbb{E}_{x \sim p_{actual}} [q_\phi(z|x)]$.

The original VAE [23] uses KL-divergence in Eqn 9, and thus optimizes the objective:

$$\mathcal{L}_{VAE} = -\gamma \mathbb{E}_{x \sim p} [KL(q_\phi(z|x)||p(z))] + \mathbb{E}_{x \sim p} \mathbb{E}_{z \sim q_\phi(z|x)} [\log(p_\theta(x|z))] \quad (10)$$

where p is p_{actual} . However, using KL-divergence in Eqn 9 has some shortcomings. As pointed out by [10,39,58], the KL-divergence in Eqn 10 can be restrictive [11,40,6] as it encourages the encoding $q_\phi(z|x)$ to be a random sample from $p(z)$ for each x , making them uninformative about the input. Also, it is not strong enough a regularizer compared to the reconstruction loss and tends to overfit data, consequently, learning a $q_\phi(z|x)$ that has high variance. Both the aforementioned shortcomings can affect the encoding distribution by making them uninformative of inputs with high variance. Since we use VAEs to better capture a linear latent manifold and subsequently define interpolations there, a bad latent distribution can affect our method significantly. We hence use a variant *Maximum Mean Discrepancy VAE* (MMD-VAE)[58] which uses a MMD Loss [15] instead of KL-divergence, and hence optimizes the objective:

$$\mathcal{L}_{MMD-VAE} = \gamma \cdot MMD(q_\phi(z)||p(z)) + \mathbb{E}_{x \sim p_{actual}} \mathbb{E}_{z \sim q_\phi(z|x)} [\log(p_\theta(x|z))] \quad (11)$$

A MMD-VAE doesn't suffer from the aforementioned shortcomings [58], as it maximizes mutual information between x and z by matching the distribution over encodings $q_\phi(z)$ with prior $p(z)$ only in expectation, rather than for every input. We hence train an MMD-VAE to characterize the training distribution more effectively. We now define a Mixup vicinal distribution in the latent space of the trained VAE as:

$$\begin{aligned} v_{VarMixup}(z, y|x_i, y_i) &= \frac{1}{n} \cdot \sum_{j=1}^N \mathbb{E}_\lambda [\delta(z = \lambda \cdot \mathbb{E}_z[q_\phi(z|x_i)] + (1 - \lambda) \cdot \mathbb{E}_z[q_\phi(z|x_j)]], \\ y &= \lambda \cdot y_i + (1 - \lambda) \cdot y_j] \end{aligned} \quad (12)$$

where $\lambda \sim \beta(\eta, \eta)$ and $\eta > 0$. Using the above vicinal distribution, $v_{VarMixup}$ and the MMD-VAE decoder, $p_\theta(x|z)$, we construct VarMixup samples as:

$$\begin{aligned} x' &= \mathbb{E}_x [p_\theta(x|\lambda \cdot \mathbb{E}_z[q_\phi(z|x_i)] + (1 - \lambda) \cdot \mathbb{E}_z[q_\phi(z|x_j)])] \\ y' &= \lambda \cdot y_i + (1 - \lambda) \cdot y_j \end{aligned}$$

From another perspective, one could view our new sampling technique as performing Manifold Mixup [46], however over the latent space of an MMD-VAE

(instead of the neural network feature space) and using it for sample reconstruction. (We compare against Manifold Mixup in our results.) Figure 2 illustrates the conceptual idea behind VarMixup.

Analogous to the empirical distribution, p_δ used in Eqn 4, we also define a (non-vicinal) Empirical Risk Minimization, defined using the VAE, which we call VarERM, and is given by:

$$p_{VarERM}(z, y) = \frac{1}{N} \cdot \sum_{i=1}^N \delta(z = \mathbb{E}_z[q_\phi(z|x_i)], y = y_i) \quad (13)$$

and use the MMD-VAE decoder, $p_\theta(x|z)$ to construct samples which are close to the original distribution. We use this for comparisons in our experiments.

Additionally, it is easy to observe that our VarMixup sampling can also be integrated with Mixup-Inference which is given by:

$$F_w^{MI}(x) = \mathbb{E}_{x_s \sim \rho_{MI}} F_w(\mathbb{E}_x[p_\theta(x|\lambda_{MI} \cdot \mathbb{E}_z[q_\phi(z|x)] + (1 - \lambda_{MI}) \cdot \mathbb{E}_z[q_\phi(z|x_s)])]) \quad (14)$$

We call this modified Mixup-Inference as VarMI (Variational Mixup Inference) in our experiments and show that under oblivious attacks, VarMixup and VarMI together performs significantly better than regular Mixup + MI and other adversarial training baselines.

4 Experiments and Results

We now present our experimental studies and results using our method, VarMixup, on multiple datasets. We begin by describing the datasets, evaluation criteria and implementation details.

Datasets: We perform experiments on four well-known standard datasets: CIFAR-10, CIFAR-100 [24], SVHN [32] and Tiny-ImageNet [13]. Descriptions of these standard datasets are deferred to the Supplementary section. *CIFAR-10* is a subset of 80 million tiny images dataset and consists of 60,000 32×32 color images containing one of 10 object classes, with 6000 images per class. *CIFAR-100* is just like CIFAR-10, except that it has 100 classes containing 600 images each. There are 500 training images and 100 testing images per class. *SVHN* is obtained from house numbers in Google Street View images. It consists of 32×32 color images belonging to 10 classes with 73257 digits for training and 26032 digits for testing. *Tiny-Imagenet* has 200 classes, with each class containing 500 training images, 50 validation images, and 50 test images. Each image here is of resolution 64×64 .

Evaluation Criteria: Analogous to Mixup Inference [33], we evaluate trained models under the oblivious setting [9] where the adversary is not aware of the existence of the defense mechanism (e.g. MI, VarMI), and generates adversarial examples based on the classification model. We follow recent papers [33,38,25,31] and use a 10-step untargeted PGD [27] attack with step-size $\alpha = \frac{8}{255}$ and l_∞ perturbation $\epsilon = \frac{8}{255}$ across all datasets. We also report accuracy on clean images and standard deviations over 10 trials. We evaluate the robustness of our trained models on the newer CIFAR-10-C, CIFAR-100-C and Tiny-Imagenet-C datasets [18] too. These datasets contain images, corrupted with 15 different distortions

at 5 severity levels. Additionally, We also perform evaluation under white-box adaptive setting [2] analogous to Mixup-Inference. In section 5, we also evaluate our models on targeted, stronger PGD and gradient-free attacks to confirm the absence of gradient masking or obfuscation [7,2].

Implementation Details: It has been shown [22] that training a network adversarially removes irrelevant biases (e.g. texture biases) in their hidden representations, thus making them more informative. We hence hypothesize that the considered VAE, if trained adversarially, will have more informative latent encoding than its regular equivalent. This would hence help improve the empirical/vicinal distributions like VarMixup, VarERM and VarMI. Empirically, we validate this hypothesis in our subsequent experiments and use prefix *adv*- (eg: *adv*-VarMixup) to distinguish them from their regular variants. We stress that the aforementioned approach should not be confused with training a model adversarially using VarMixup (we only train the VAE adversarially). We also train a model adversarially using VarMixup, but discuss these results in the Supplementary section to avoid overcrowding of results and space constraints. Table 1 summarizes the variants of our approach that we consider with their corresponding abbreviations, which we used in subsequent sections. All models are trained on Resnet-34 [17] backbone across all datasets. A study on varying hyper-parameters is presented in Section 5.

Table 1: Variants of our approach and their implementation details. reg - regular, adv-adversarial, MI- Mixup Inference

VAE	Method	MI	Abbreviation	Details
reg. adv.	ERM	No	VarERM <i>adv</i> -VarERM	Variational ERM (Eqn 13), Adam Optimizer ($lr = 1e - 3$), 100 epochs
reg. adv.	ERM	Yes	VarERM + VarMI <i>adv</i> -VarERM + <i>adv</i> -VarMI	Inference using Variational MI (Eqn 14), $\lambda_{MI} = 0.5$ and $N_{MI} = 30$.
reg. adv.	Mixup	No	VarMixup <i>adv</i> -VarMixup	VarMixup (Eqn 12), Adam Optimizer ($lr = 1e - 3$), 150 epochs, Mixup coefficient sampled from $\beta(1, 1)$
reg. adv.	Mixup	Yes	VarMixup + VarMI <i>adv</i> -VarMixup + <i>adv</i> -VarMI	Inference using Variational MI (Eqn 14), $\lambda_{MI} = 0.5$ and $N_{MI} = 30$.

Baseline Models: We compare our methods against an exhaustive set of baselines including non-VRM variants, mixup variants and state-of-the-art adversarial techniques. Below are their details:

1. *ERM* - Vanilla Empirical Risk Minimization (Eqn 4) using Adam optimizer ($lr = 1e - 3$) for 100 epochs on all datasets.
2. *ERM + MI* - Using Mixup-Inference [33] (MI-OL) on *ERM* with $\lambda_{MI} = 0.5$ and $N_{MI} = 30$.
3. *Mixup* - Vanilla Mixup training [57] using Adam optimizer ($lr = 1e - 3$) for 150 epochs on all datasets. Mixup coefficient is sampled from $\beta(1, 1)$.
4. *Mixup + MI* - Using Mixup-Inference [33] (MI-OL) on *Mixup* with $\lambda_{MI} = 0.5$ and $N_{MI} = 30$.
5. *AT and TRADES* - l_∞ PGD/TRADES adversarial training [27,56] with $\epsilon = 8/255$ and step-size $\alpha = 2/255$. Models are trained using Adam optimizer ($lr = 1e - 3$) for 250 epochs on all datasets.

6. *IAT* - l_∞ Interpolated adversarial training [25] with $\epsilon = 8/255$ and step-size $\alpha = 2/255$. Interpolation coefficient is sampled from $\beta(1, 1)$. Models are trained using Adam optimizer ($lr = 1e - 3$) for 350 epochs on all datasets.
7. *IAT + MI* - Using Mixup-Inference [33] (MI-OL) on *IAT* with $\lambda_{MI} = 0.6$ and $N_{MI} = 30$.
8. *LAT, LLR and CURE* - Adversarial training methods: Latent adversarial training [38], Local-Linear Regularization [35] and Curvature regularization [31] reported from original papers.

Robustness on CIFAR-10, CIFAR-100, SVHN and Tiny-Imagenet: We first evaluate the robustness and report our results in Table 2. As can be seen, without any adversarial training *VarMixup + VarMI* outperforms state-of-the-art adversarial training techniques by a significant margin ($\sim 5\%$ over *IAT + MI* and $\sim 10 - 12\%$ over other AT techniques). Also, it can be noticed that the adversarial variant of our approach - *adv-VarMixup + adv-VarMI* performs better across all datasets.

Transferability from Tiny-Imagenet to CIFAR-10 and CIFAR-100: The proposed methodology will be more scalable and time-efficient, if a VAE trained on a dataset such as ImageNet can be used to generate *VarMixup* samples for other datasets. This is a typical transfer learning setting, and we study the performance of training *VarMixup* models on CIFAR-10 and CIFAR-100 datasets using MMD-VAE trained on the Tiny-Imagenet dataset. We report our findings in Table 3. It can be seen that our approaches - *VarMixup + VarMI/adv-VarMixup + adv-VarMI* still manage to outperform all adversarial training baselines (which are trained directly on the target dataset) by a good margin ($\sim 1 - 2\%$ over *IAT+MI* and $\sim 10 - 15\%$ over other AT techniques).

Robustness to common input corruptions: Apart from adversarial perturbations, we also evaluate the trained models on various common input corruptions. Hendrycks et al. [18] recently proposed newer CIFAR-10, CIFAR-100 and Tiny-Imagenet test datasets (CIFAR-10-C, CIFAR-100-C, and Tiny-Imagenet-C) containing images corrupted with 15 different distortions (Gaussian blur, Shot Noise, Impulse Noise, JPEG compression, Motion blur, frost, etc.) and 5 levels of severity. We report the mean classification accuracy over all distortions on CIFAR-10-C, CIFAR-100-C and Tiny-Imagenet-C datasets in Table 4. From the table, our method - *VarMixup/adv-VarMixup* achieves superior performance by a margin of $\sim 2 - 4\%$. It is also interesting to note that other variants like *VarERM/adv-VarERM* also perform significantly better than vanilla ERM and many adversarial training techniques, highlighting our method’s effectiveness.

Comparison with Manifold Mixup: As stated in Section 3, one could view our method as performing Manifold Mixup in a latent space. It has been stated [46] that models trained using Manifold Mixup are not robust to strong adversarial attacks like PGD [27]. However, for completeness and fairness, we study the performance of the two approaches. We obtain 2.24% and 9.48% accuracy against a 10-step PGD attack (used in Table 2) using Manifold-Mixup and Manifold-Mixup + MI on the CIFAR-10 dataset. For CIFAR-100, the corresponding accuracies are 1.87% and 5.94% on Manifold-Mixup and Manifold-Mixup + MI respectively. For SVHN, Manifold mixup achieves adversarial accuracy 26.5%

Table 2: Robustness against PGD attack on CIFAR-10, CIFAR-100, SVHN and Tiny-Imagenet datasets. Best results in **bold** and second best underlined. '-' denotes no implementation or results available. Original (clean) accuracy of each model (w/o adversarial perturbations) reported in parentheses.

Method	PGD ₁₀ (Clean)	
	CIFAR-10	CIFAR-100
AT [27]	47.34 \pm 0.32 (85.58 \pm 0.14)	22.72 \pm 0.37 (60.28 \pm 0.13)
LAT [38]	53.84 (87.80)	27.03 (60.94)
IAT [25]	40.0 \pm 0.57 (89.7 \pm 0.33)	20.6 \pm 0.49 (62.7 \pm 0.21)
TRADES [56]	51.65 \pm 0.32 (88.11 \pm 0.43)	25.5 \pm 0.35 (63.3 \pm 0.32)
LLR [35]	54.95 (86.83)	-
CURE [31]	47.69 (84.45)	-
IAT + MI [33]	61.57 \pm 1.30 (84.2 \pm 1.26)	30.85 \pm 1.04 (61.4 \pm 1.15)
ERM	0.0 \pm 0.0 (94.5 \pm 0.14)	0.0 \pm 0.01 (64.5 \pm 0.10)
VarERM	0.27 \pm 0.07 (90.22 \pm 0.43)	0.7 \pm 0.04 (63.28 \pm 0.46)
<i>adv</i> -VarERM	1.01 \pm 0.02 (88.47 \pm 0.39)	0.56 \pm 0.05 (62.74 \pm 0.26)
Mixup [57]	7.5 \pm 0.32 (95.5 \pm 0.35)	0.36 \pm 0.12 (76.8 \pm 0.41)
VarMixup	12.34 \pm 0.37 (91.91 \pm 0.45)	0.72 \pm 0.12 (67.2 \pm 0.44)
<i>adv</i> -VarMixup	17.66 \pm 0.23 (89.19 \pm 0.32)	0.74 \pm 0.19 (67.13 \pm 0.34)
ERM + MI	12.4 \pm 1.02 (60.23 \pm 0.97)	2.4 \pm 1.11 (35.46 \pm 0.92)
VarERM + VarMI	30.49 \pm 1.03 (56.38 \pm 1.0)	12.04 \pm 0.98 (33.88 \pm 1.10)
<i>adv</i> -VarERM + <i>adv</i> -VarMI	38.13 \pm 1.09 (53.30 \pm 0.95)	11.45 \pm 1.01 (31.79 \pm 1.20)
Mixup + MI [33]	25.76 \pm 1.12 (86.84 \pm 1.05)	6.71 \pm 1.03 (67.8 \pm 1.06)
VarMixup + VarMI	66.84 \pm 1.08 (82.15 \pm 0.92)	35.8 \pm 1.24 (63.5 \pm 1.34)
<i>adv</i> -VarMixup + <i>adv</i> -VarMI	68.66 \pm 1.21 (82.06 \pm 1.19)	40.13 \pm 1.2 (63.98 \pm 1.32)
Method	PGD ₁₀ (Clean)	
	SVHN	Tiny-Imagenet
AT [27]	54.58 \pm 0.53 (91.88 \pm 0.34)	3.78 \pm 0.21 (22.33 \pm 0.16)
LAT [38]	60.23 (91.65)	-
IAT [25]	54.83 \pm 0.67 (93.41 \pm 0.47)	12.13 \pm 0.18 (51.94 \pm 0.28)
TRADES [56]	-	3.83 \pm 0.12 (26.12 \pm 0.38)
CURE [31]	32.43 \pm 0.02 (79.28 \pm 0.01)	-
IAT + MI [33]	60.0 \pm 1.09 (80.0 \pm 1.34)	12.1 \pm 0.24 (18.08 \pm 0.34)
ERM	0.45 \pm 0.11 (95.47 \pm 0.56)	0.0 \pm 0.0 (49.96 \pm 0.12)
VarERM	0.67 \pm 0.23 (95.60 \pm 0.55)	0.1 \pm 0.03 (46.35 \pm 0.36)
<i>adv</i> -VarERM	0.17 \pm 0.08 (95.10 \pm 0.56)	0.04 \pm 0.01 (43.87 \pm 0.27)
Mixup	4.28 \pm 0.52 (96.54 \pm 0.49)	0.0 \pm 0.0 (53.83 \pm 0.17)
VarMixup	2.59 \pm 0.50 (96.72 \pm 0.48)	0.01 \pm 0.01 (46.98 \pm 0.11)
<i>adv</i> -VarMixup	3.38 \pm 0.53 (95.64 \pm 0.50)	0.0 \pm 0.0 (46.58 \pm 0.23)
ERM + MI	37.00 \pm 0.98 (71.85 \pm 1.21)	1.54 \pm 0.05 (25.56 \pm 0.83)
VarERM + VarMI	38.25 \pm 0.99 (66.93 \pm 1.20)	5.8 \pm 0.14 (23.61 \pm 0.72)
<i>adv</i> -VarERM + <i>adv</i> -VarMI	53.81 \pm 1.05 (69.78 \pm 1.29)	7.27 \pm 0.19 (25.73 \pm 0.77)
Mixup + MI	37.05 \pm 1.30 (89.97 \pm 1.34)	2.93 \pm 0.5 (47.2 \pm 0.23)
VarMixup + VarMI	<u>78.08 \pm 1.05</u> (88.45 \pm 1.11)	<u>12.75 \pm 0.42</u> (42.88 \pm 0.15)
<i>adv</i> -VarMixup + <i>adv</i> -VarMI	87.20 \pm 1.09 (88.40 \pm 1.12)	19.9 \pm 0.53 (44.18 \pm 0.24)

Table 3: Transferability results on CIFAR-10 and CIFAR-100. Best results in **bold** and second best underlined. '-' denotes no implementation or results available. Original clean accuracy reported in parentheses.

Method	PGD ₁₀ (Clean)	
	CIFAR-10	CIFAR-100
AT [27]	47.34 \pm 0.32 (85.58 \pm 0.14)	22.72 \pm 0.37 (60.28 \pm 0.13)
LAT [38]	53.84 (87.80)	27.03 (60.94)
IAT [25]	40.0 \pm 0.57 (89.7 \pm 0.33)	20.6 \pm 0.49 (62.7 \pm 0.21)
TRADES [56]	51.65 \pm 0.32 (88.11 \pm 0.43)	25.5 \pm 0.35 (63.3 \pm 0.32)
LLR [35]	54.95 (86.83)	-
CURE [31]	47.69 (84.45)	-
IAT + MI [33]	61.57 \pm 1.30 (84.2 \pm 1.26)	30.85 \pm 1.04 (61.4 \pm 1.15)
ERM	0.0 \pm 0.0 (94.5 \pm 0.14)	0.0 \pm 0.01 (64.5 \pm 0.10)
VarERM	0.12 \pm 0.01 (90.34 \pm 0.23)	0.54 \pm 0.05 (63.4 \pm 0.33)
adv-VarERM	0.37 \pm 0.19 (89.89 \pm 0.12)	0.66 \pm 0.04 (62.08 \pm 0.17)
Mixup	7.5 \pm 0.32 (95.5 \pm 0.35)	0.36 \pm 0.12 (76.8 \pm 0.41)
VarMixup	10.21 \pm 0.34 (91.09 \pm 0.21)	0.82 \pm 0.14 (67.7 \pm 0.27)
adv-VarMixup	8.33 \pm 0.11 (90.71 \pm 0.31)	0.44 \pm 0.09 (65.48 \pm 0.43)
ERM + MI	12.4 \pm 1.02 (60.23 \pm 0.97)	2.4 \pm 1.11 (35.46 \pm 0.92)
VarERM + VarMI	24.46 \pm 1.23 (52.12 \pm 1.01)	12.0 \pm 1.09 (34.84 \pm 0.98)
adv-VarERM + adv-VarMI	31.96 \pm 1.1 (58.94 \pm 0.96)	13.02 \pm 1.13 (33.04 \pm 0.92)
MT + MI	25.76 \pm 1.12 (86.84 \pm 1.05)	6.71 \pm 1.03 (67.8 \pm 1.06)
VarMixup + VarMI	62.26 \pm 1.11 (82.48 \pm 1.12)	30.3 \pm 1.03 (60.03 \pm 0.99)
adv-VarMixup + adv-VarMI	63.41 \pm 1.20 (82.76 \pm 1.02)	31.3 \pm 1.15 (60.74 \pm 0.95)

and 11.55% with and without MI. For Tiny Imagenet, the accuracies are 2.99% and 0.07% for Manifold Mixup with and without MI respectively. As can be compared from Table 2, VarMixup + MI performs superior to Manifold Mixup. We defer analogous results on SVHN and Tiny-Imagenet datasets to the Supplementary material due to space constraints. Our results show that the use of the latent unfolded manifold is indeed better than using hidden layer representations.

Performance under White-box Adaptive Attacks: Following Athalye et al. [2] and analogous to Mixup-Inference [33], we design adaptive white-box attacks for VarMI. From Eqn 14, VarMI is given as:

$$F_w^{VarMI}(x) = \mathbb{E}_{\rho_{MI}} F_w(\mathbb{E}_x[p_\theta(x|\lambda_{MI} \cdot \mathbb{E}_z[q_\phi(z|x)] + (1 - \lambda_{MI}) \cdot \mathbb{E}_z[q_\phi(z|x_s)])])$$

Let

$$u = \mathbb{E}_x[p_\theta(x|\lambda_{MI} \cdot \mathbb{E}_z[q_\phi(z|x)] + (1 - \lambda_{MI}) \cdot \mathbb{E}_z[q_\phi(z|x_s)])]$$

and

$$v = \lambda_{MI} \cdot \mathbb{E}_z[q_\phi(z|x)] + (1 - \lambda_{MI}) \cdot \mathbb{E}_z[q_\phi(z|x_s)]$$

Then, the gradient of VarMI prediction w.r.t. input x is given as (here, λ_{MI} is fixed throughout inference):

$$\begin{aligned}
\frac{\partial F_w^{VarMI}(x)}{\partial x} &= \mathbb{E}_{\rho_{MI}} \frac{\partial F_w(u)}{\partial x} \\
&= \mathbb{E}_{\rho_{MI}} \frac{\partial F_w(u)}{\partial u} \cdot \frac{\partial u}{\partial x} = \mathbb{E}_{\rho_{MI}} \frac{\partial F_w(u)}{\partial u} \cdot \frac{\partial u}{\partial v} \cdot \frac{\partial v}{\partial x} \\
&= \lambda_{MI} \cdot \mathbb{E}_{\rho_{MI}} \cdot \frac{\partial F_w(u)}{\partial u} \cdot \frac{\partial u}{\partial v} \cdot \frac{\partial q_\phi(z|x)}{\partial x}
\end{aligned} \tag{15}$$

Now, according to Eqn 15 above, the sign of gradients used in adaptive PGD can be approximated by:

$$\text{sign}\left(\frac{\partial F_w^{VarMI}(x)}{\partial x}\right) = \text{sign}\left(\sum_{i=1}^{N_A} \frac{\partial F_w(u)}{\partial u} \cdot \frac{\partial u}{\partial v} \cdot \mathbb{E}_z \frac{\partial q_\phi(z|x)}{\partial x}\right) \quad (16)$$

Here, the number of adaptive samples, N_A , refers to the execution times of sampling x_s in each iteration step of adaptive PGD to approximate the above equation. Figure 3 shows the performance of Mixup/VarMixup/*adv*-VarMixup under adaptive PGD attacks on CIFAR-10/-100. As can be seen, our proposed inference VarMI along with VarMixup performs better than regular Mixup and Mixup-Inference.

Table 4: Robustness to common input corruptions on CIFAR-10-C, CIFAR-100-C and Tiny-Imagenet-C [18] datasets. Best results in **bold** and second best underlined.

Method	CIFAR-10-C	CIFAR-100-C	Tiny-Imagenet-C
AT [27]	73.12 \pm 0.31	45.09 \pm 0.31	15.74 \pm 0.36
TRADES [27]	75.46 \pm 0.21	45.98 \pm 0.41	16.20 \pm 0.23
IAT [25]	81.05 \pm 0.42	50.71 \pm 0.25	18.69 \pm 0.45
ERM	69.29 \pm 0.21	47.3 \pm 0.32	17.34 \pm 0.27
VarERM	79.66 \pm 0.12	49.26 \pm 0.31	20.18 \pm 0.11
<i>adv</i> -VarERM	79.73 \pm 0.13	50.49 \pm 0.26	21.62 \pm 0.09
MT	74.74 \pm 0.34	52.13 \pm 0.43	21.55 \pm 0.37
VarMixup	82.57 \pm 0.42	52.57 \pm 0.39	24.87 \pm 0.32
<i>adv</i> -VarMixup	<u>82.12 \pm 0.46</u>	54.0 \pm 0.41	25.36 \pm 0.21

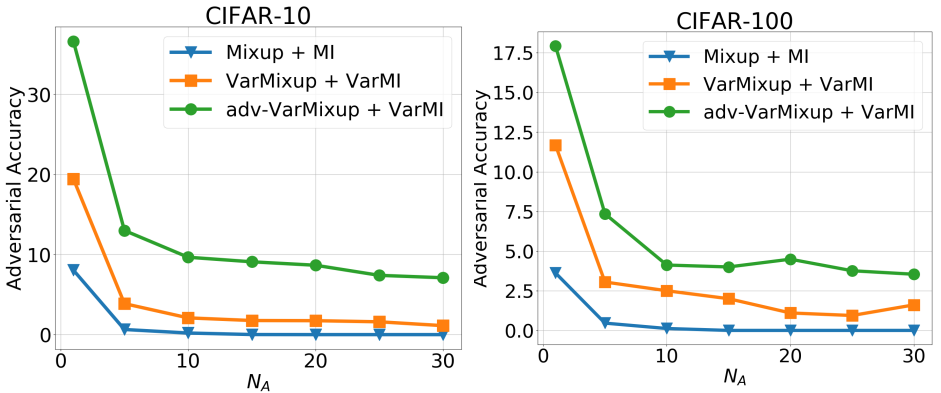


Fig. 3: Performance under 10-step adaptive PGD attacks ($\epsilon = 8/255$) on CIFAR-10 and CIFAR-100.

5 Discussion and Ablation studies

In this section, we conduct ablations to empirically characterize and analyze the efficacy of the proposed method.

Local linearity on loss landscapes: It has been shown [35] that local linearity of loss landscapes of neural networks is related to model robustness. The more the loss landscapes are linear, the more the adversarial robustness. To this fact, we analyze the local linearity of loss landscapes of VarMixup and regular mixup trained models. Qin et al. [35] defines local linearity at a data-point x within a neighbourhood $B(\epsilon)$ as: $\gamma(\epsilon, x, y) = \max_{\delta \in B(\epsilon)} |\mathcal{L}(F_w(x + \delta), y) - \mathcal{L}(F_w(x), y) - \delta^T \nabla_x \mathcal{L}(F_w(x), y)|$. Figure 4 shows the average local linear error (over test set) with increasing L_∞ max-perturbation ϵ on CIFAR-10 and CIFAR-100 datasets. As can be seen, VarMixup/*adv*-VarMixup makes the local linear error significantly ($\times 2$) lesser as compared to regular mixup, thus inducing robustness. This robustness gets further boosted by using VarMI at inference stage.

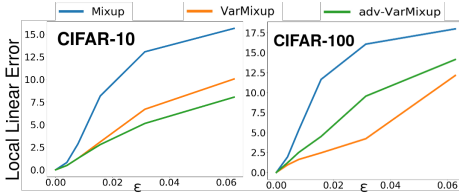


Fig. 4: Local linear error of loss landscapes of models trained on CIFAR-10/-100

regular training data and training data generated by mixup/VarMixup/ *adv*-VarMixup. These scores summarize how similar the two groups are in terms of statistics on computer vision features of the raw images calculated using the Inceptionv3 model used for image classification. Lower scores indicate the two groups of images are more similar, or have more similar statistics, with a perfect score being 0.0 indicating that the two groups of images are identical. Figure 5 reports these metrics on CIFAR-10 and CIFAR-100 respectively. The greater FID and KID scores indicate that we are adding off-manifold samples (manifold characterized by training data) to the training using our approach.

Calibration error: A recent study [42] showed that DNNs trained with Mixup are significantly better calibrated than DNNs trained in a regular fashion. Calibration [16] measures how good softmax scores are as indicators of the actual likelihood of a correct prediction. We measure the *Expected Calibration Error (ECE)* [42,16] of our trained networks, following [42]: predictions (total N predictions) are grouped into M interval bins (B_m) of equal size. The accuracy and confidence of B_m are defined as:

$$acc(B_m) = \frac{1}{|B_m|} \sum_{i \in B_m} 1 \cdot (\hat{y}_i = y_i)$$

Analyzing VarMixup samples:

Figure 7 shows sample data generated by regular Mixup, VarMixup, and *adv*-VarMixup on two images. We observe that though mixup or VarMixup samples look perceptually similar, they are quite different at statistical level. We measure the Frechet Inception Distance (FID) [20] and Kernel Inception Distance [5] between

and

$$\text{conf}(B_m) = \frac{1}{|B_m|} \sum_{i \in B_m} \hat{p}_i$$

where \hat{p}_i , \hat{y}_i , y_i are the confidence, predicted label and true label of sample i respectively. The *Expected Calibration Error*(ECE) is then defined as:

$$\text{ECE} = \sum_{m=1}^M \frac{|B_m|}{N} \cdot | \text{acc}(B_m) - \text{conf}(B_m) |$$

Models trained on CIFAR-10 with VarMixup and *adv*-VarMixup have ECE of 0.105 and 0.07 respectively whereas, model trained using regular mixup has ECE 0.13. On CIFAR-100 the ECEs are 0.135, 0.127 and 0.122 for Mixup, VarMixup and *adv*-VarMixup models respectively. This indicates that our VarMixup models are better calibrated than regular Mixup.

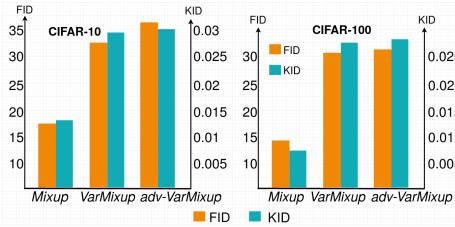


Fig. 5: FID and KID scores between training set and mixup/VarMixup generated samples on CIFAR-10 and CIFAR-100

VarMixup on Interpolated Adversarial Training:

We also integrate VarMixup with the more recent Interpolated Adversarial Training (IAT) [25], and call it *VarIAT*. On CIFAR-10, VarIAT and VarIAT+VarMI achieve adversarial robustness of 49.37% and 71.7%, respectively. For SVHN, the adversarial accuracies are 21.07% and 81.18% for VarIAT and VarIAT+VarMI, respectively. As can be seen from Table 2 (main sub-mission), under oblivious settings,

VarIAT (VarIAT + VarMI) achieves superior performance to IAT (IAT + MI) in most scenarios. The evaluations were carried out in the same setting as Table 2.

Robustness to stronger, targeted and gradient-free attacks: we also evaluate our models on a stronger 50-step PGD attack [27] (PGD₅₀), targeted 10-step PGD attacks (t-PGD₁₀) and Gradient free SPSA [45] attack. We use $\epsilon = 8/255$ for all attacks. For targeted attacks, we chose the second most likely class as target class. SPSA results are evaluated over 1000 test samples. We report our results in Table 5. As can be seen, our methods VarMixup + VarMI outperforms the rest in most scenarios. The results also confirm the absence of any gradient masking and obfuscation [7,2] in our training method.

Hyperparameter variations: We vary the beta distribution $\beta(\eta, \eta)$ (used to sample Mixup coefficient) parameter - η and train models using mixup, VarMixup and *adv*-VarMixup and plot their adversarial accuracies in Figure 6. Figure 6 shows the variation of adversarial accuracy when λ_{MI} is varied from 0 to 1 in MI or VarMI. Both figures show that our VarMixup trained models perform better irrespective of hyperparameters in most cases.

Table 5: Robustness against stronger PGD, targeted and SPSA attacks [45] on CIFAR-10 and CIFAR-100 datasets. Best results in **bold** and second best underlined.

Method	CIFAR-10			CIFAR-100		
	PGD ₅₀	t-PGD ₁₀	SPSA	PGD ₅₀	t-PGD ₁₀	SPSA
MT + MI [33]	11.29	48.28	69.28	3.61	31.83	46.42
VarMixup + VarMI	<u>65.11</u>	77.59	76.34	<u>35.14</u>	<u>53.32</u>	<u>60.32</u>
<i>adv</i> -VarMixup + <i>adv</i> -VarMI	67.34	<u>75.29</u>	72.66	40.01	54.81	61.02
AT [27]	46.4	49.49	79.68	21.56	34.56	53.60
IAT [25]	34.04	49.04	84.41	18.08	28.2	59.82
TRADES [56]	50.24	50.01	<u>81.07</u>	34.78	33.6	48.65
IAT + MI [33]	60.84	68.70	76.06	29.5	36.52	45.3

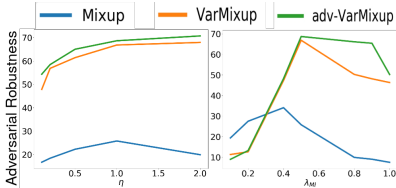


Fig. 6: (a) Varying η in $\beta(\eta, \eta)$ distribution from where mixup coefficient is sampled, (b) Variation of hyper-parameter λ_{MI} in MI or VarMI.

Computational Overhead: We compare the computational time of our trained models using VarMixup/*adv*-VarMixup with AT and TRADES adversarial training techniques. VarMixup, *adv*-VarMixup, AT and TRADES take around 3, 5, 8.8 and 15 hours respectively. We considered the MMD-VAE training time too in these results. In addition, the transferability of a VAE trained on one dataset to do VarMixup on another makes our approach time-efficient and scalable.

6 Conclusions

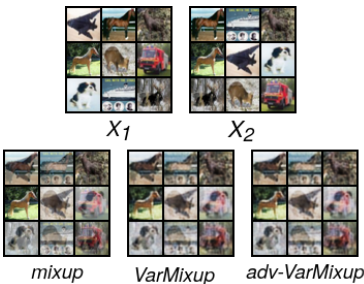


Fig. 7: Samples generated by mixup, VarMixup and *adv*-VarMixup on CIFAR-10 (Mixup coefficient $\lambda = 0.5$).

In this work, we propose a Mixup vicinal distribution, VarMixup, which performs linear interpolations on an unfolded latent manifold where linearity in between training examples is likely to be preserved by construction. Analogous to Mixup Inference, we also define Variational Mixup Inference (VarMI) which when combined with VarMixup trained models provides significant gains in adversarial robustness over regular Mixup, Mixup Inference, and state-of-the-art adversarial training techniques under oblivious attacks. We also show that VarMixup trained models are more robust to common input corruptions, are better calibrated and have significantly lower local-linear loss than regular mixup models. Additionally, our experiments indicate that VarMixup adds more off-manifold images to training than regular mixup, which we believe is the primary reason for observed robustness. Our work highlights the efficacy of defining vicinal distributions by using neighbors on unfolded latent manifold rather than data manifold and we believe that our work can open a discussion around this notion of robustness and choice of vicinal distributions.

References

1. Alexey Kurakin, Ian J. Goodfellow, S.B.: Adversarial examples in the physical world. ICLR Workshop (2017)
2. Athalye, A., Carlini, N., Wagner, D.A.: Obfuscated gradients give a false sense of security: Circumventing defenses to adversarial examples. CoRR **abs/1802.00420** (2018), <http://arxiv.org/abs/1802.00420>
3. Beckham, C., Honari, S., Verma, V., Lamb, A.M., Ghadiri, F., Hjelm, R.D., Bengio, Y., Pal, C.: On adversarial mixup resynthesis. In: Advances in Neural Information Processing Systems 32, pp. 4346–4357. Curran Associates, Inc. (2019), <http://papers.nips.cc/paper/8686-on-adversarial-mixup-resynthesis.pdf>
4. Berthelot, D., Carlini, N., Goodfellow, I., Papernot, N., Oliver, A., Raffel, C.A.: Mixmatch: A holistic approach to semi-supervised learning. In: Advances in Neural Information Processing Systems 32, pp. 5049–5059. Curran Associates, Inc. (2019), <http://papers.nips.cc/paper/8749-mixmatch-a-holistic-approach-to-semi-supervised-learning.pdf>
5. Bikowski, M., Sutherland, D.J., Arbel, M., Gretton, A.: Demystifying MMD GANs. In: International Conference on Learning Representations (2018), <https://openreview.net/forum?id=r1lU0zWCW>
6. Bowman, S.R., Vilnis, L., Vinyals, O., Dai, A., Jozefowicz, R., Bengio, S.: Generating sentences from a continuous space. In: Proceedings of The 20th SIGNLL Conference on Computational Natural Language Learning. pp. 10–21. Association for Computational Linguistics, Berlin, Germany (Aug 2016). <https://doi.org/10.18653/v1/K16-1002>, <https://www.aclweb.org/anthology/K16-1002>
7. Carlini, N., Athalye, A., Papernot, N., Brendel, W., Rauber, J., Tsipras, D., Goodfellow, I.J., Madry, A., Kurakin, A.: On evaluating adversarial robustness. CoRR **abs/1902.06705** (2019), <http://arxiv.org/abs/1902.06705>
8. Carlini, N., Wagner, D.: Towards evaluating the robustness of neural networks. In: 2017 IEEE Symposium on Security and Privacy (SP) (2017)
9. Carlini, N., Wagner, D.A.: Adversarial examples are not easily detected: Bypassing ten detection methods. CoRR **abs/1705.07263** (2017), <http://arxiv.org/abs/1705.07263>
10. Chen, X., Kingma, D.P., Salimans, T., Duan, Y., Dhariwal, P., Schulman, J., Sutskever, I., Abbeel, P.: Variational lossy autoencoder. CoRR **abs/1611.02731** (2016), <http://arxiv.org/abs/1611.02731>
11. Chen, X., Kingma, D.P., Salimans, T., Duan, Y., Dhariwal, P., Schulman, J., Sutskever, I., Abbeel, P.: Variational lossy autoencoder. CoRR **abs/1611.02731** (2016), <http://arxiv.org/abs/1611.02731>
12. Cisse, M., Bojanowski, P., Grave, E., Dauphin, Y., Usunier, N.: Parseval networks: Improving robustness to adversarial examples. In: Precup, D., Teh, Y.W. (eds.) Proceedings of the 34th International Conference on Machine Learning. Proceedings of Machine Learning Research, vol. 70, pp. 854–863. PMLR, International Convention Centre, Sydney, Australia (06–11 Aug 2017), <http://proceedings.mlr.press/v70/cisse17a.html>
13. CS231N, S.: Tiny ImageNet Visual Recognition Challenge, <https://tiny-imagenet.herokuapp.com/>
14. Goodfellow, I., Shlens, J., Szegedy, C.: Explaining and harnessing adversarial examples. In: International Conference on Learning Representations (2015), <http://arxiv.org/abs/1412.6572>

15. Gretton, A., Borgwardt, K., Rasch, M., Schölkopf, B., Smola, A.J.: A kernel method for the two-sample-problem. In: Schölkopf, B., Platt, J.C., Hoffman, T. (eds.) *Advances in Neural Information Processing Systems 19*, pp. 513–520. MIT Press (2007), <http://papers.nips.cc/paper/3110-a-kernel-method-for-the-two-sample-problem.pdf>
16. Guo, C., Pleiss, G., Sun, Y., Weinberger, K.Q.: On calibration of modern neural networks. CoRR **abs/1706.04599** (2017), <http://arxiv.org/abs/1706.04599>
17. He, K., Zhang, X., Ren, S., Sun, J.: Deep residual learning for image recognition. In: 2016 IEEE Conference on Computer Vision and Pattern Recognition (CVPR). pp. 770–778 (June 2016). <https://doi.org/10.1109/CVPR.2016.90>
18. Hendrycks, D., Dietterich, T.: Benchmarking neural network robustness to common corruptions and perturbations. *Proceedings of the International Conference on Learning Representations* (2019)
19. Hendrycks*, D., Mu*, N., Cubuk, E.D., Zoph, B., Gilmer, J., Lakshminarayanan, B.: Augmix: A simple method to improve robustness and uncertainty under data shift. In: *International Conference on Learning Representations* (2020), <https://openreview.net/forum?id=S1gmrxFvB>
20. Heusel, M., Ramsauer, H., Unterthiner, T., Nessler, B., Klambauer, G., Hochreiter, S.: Gans trained by a two time-scale update rule converge to a nash equilibrium. CoRR **abs/1706.08500** (2017), <http://arxiv.org/abs/1706.08500>
21. Ilyas, A., Engstrom, L., Athalye, A., Lin, J.: Black-box adversarial attacks with limited queries and information. *ICML* (2018)
22. Ilyas, A., Santurkar, S., Tsipras, D., Engstrom, L., Tran, B., Madry, A.: Adversarial examples are not bugs, they are features. In: *Advances in Neural Information Processing Systems 32*, pp. 125–136. Curran Associates, Inc. (2019), <http://papers.nips.cc/paper/8307-adversarial-examples-are-not-bugs-they-are-features.pdf>
23. Kingma, D.P., Welling, M.: Auto-encoding variational bayes. CoRR **abs/1312.6114** (2013)
24. Krizhevsky, A.: Learning multiple layers of features from tiny images (2009)
25. Lamb, A., Verma, V., Kannala, J., Bengio, Y.: Interpolated adversarial training: Achieving robust neural networks without sacrificing too much accuracy. In: *Proceedings of the 12th ACM Workshop on Artificial Intelligence and Security*. p. 95103. AISec19, Association for Computing Machinery, New York, NY, USA (2019). <https://doi.org/10.1145/3338501.3357369>, <https://doi.org/10.1145/3338501.3357369>
26. Liu, X., Zou, Y., Kong, L., Diao, Z., Yan, J., Wang, J., Li, S., Jia, P., You, J.: Data augmentation via latent space interpolation for image classification. In: 2018 24th International Conference on Pattern Recognition (ICPR). pp. 728–733 (Aug 2018). <https://doi.org/10.1109/ICPR.2018.8545506>
27. Madry, A., Makelov, A., Schmidt, L., Tsipras, D., Vladu, A.: Towards deep learning models resistant to adversarial attacks. In: *International Conference on Learning Representations* (2018), <https://openreview.net/forum?id=rJzIBfZAb>
28. Miyato, T., Maeda, S.i., Koyama, M., Nakae, K., Ishii, S.: Distributional smoothing with virtual adversarial training. *ICLR* (2016)
29. Moosavi-Dezfooli, S.M., Fawzi, A., Fawzi, O., Frossard, P.: Universal adversarial perturbations. *CVPR* (2017)
30. Moosavi-Dezfooli, S.M., Fawzi, A., Frossard, P.: Deepfool: a simple and accurate method to fool deep neural networks. *arXiv preprint arXiv:1511.04599v3* (2016)

31. Moosavi-Dezfooli, S.M., Fawzi, A., Uesato, J., Frossard, P.: Robustness via curvature regularization, and vice versa. In: *Proceedings of the IEEE Conference on Computer Vision and Pattern Recognition*. pp. 9078–9086 (2019)
32. Netzer, Y., Wang, T., Coates, A., Bissacco, A., Wu, B., Ng, A.: Reading digits in natural images with unsupervised feature learning. *NIPS* (01 2011)
33. Pang*, T., Xu*, K., Zhu, J.: Mixup inference: Better exploiting mixup to defend adversarial attacks. In: *International Conference on Learning Representations* (2020), <https://openreview.net/forum?id=ByxtC2VtPB>
34. Papernot, N., McDaniel, P., Goodfellow, I.J., Jha, S., Celik, Z.B., Swami, A.: Practical black-box attacks against machine learning. *ACM* (2017)
35. Qin, C., Martens, J., Goyal, S., Krishnan, D., Fawzi, A., De, S., Stanforth, R., Kohli, P., et al.: Adversarial robustness through local linearization. *arXiv preprint arXiv:1907.02610* (2019)
36. Samangouei, P., Kabkab, M., Chellappa, R.: Defense-gan: Protecting classifiers against adversarial attacks using generative models. *CoRR* **abs/1805.06605** (2018), <http://arxiv.org/abs/1805.06605>
37. Shafahi, A., Najibi, M., Ghiasi, A., Xu, Z., Dickerson, J.P., Studer, C., Davis, L.S., Taylor, G., Goldstein, T.: Adversarial training for free! *CoRR* **abs/1904.12843** (2019), <http://arxiv.org/abs/1904.12843>
38. Sinha, A., Singh, M., Kumari, N., Krishnamurthy, B., Machiraju, H., Balasubramanian, V.N.: Harnessing the vulnerability of latent layers in adversarially trained models. *CoRR* **abs/1905.05186** (2019), <http://arxiv.org/abs/1905.05186>
39. Sønderby, C.K., Raiko, T., Maaløe, L., Sønderby, S.K., Winther, O.: Ladder variational autoencoders. In: *Proceedings of the 30th International Conference on Neural Information Processing Systems*. p. 37453753. *NIPS16*, Curran Associates Inc., Red Hook, NY, USA (2016)
40. Sønderby, C.K., Raiko, T., Maaløe, L., Sønderby, S.K., Winther, O.: Ladder variational autoencoders. In: *Proceedings of the 30th International Conference on Neural Information Processing Systems*. p. 37453753. *NIPS16*, Curran Associates Inc., Red Hook, NY, USA (2016)
41. Szegedy, C., Zaremba, W., Sutskever, I., Bruna, J., Erhan, D., Goodfellow, I., Fergus, R.: Intriguing properties of neural networks. *arXiv preprint arXiv:1312.6199* (2013)
42. Thulasidasan, S., Chennupati, G., Bilmes, J.A., Bhattacharya, T., Michalak, S.: On mixup training: Improved calibration and predictive uncertainty for deep neural networks. In: *Advances in Neural Information Processing Systems* 32, pp. 13888–13899. Curran Associates, Inc. (2019), <http://papers.nips.cc/paper/9540-on-mixup-training-improved-calibration-and-predictive-uncertainty-for-d> pdf
43. Tsipras, D., Santurkar, S., Engstrom, L., Turner, A., Madry, A.: Robustness May Be at Odds with Accuracy. *arXiv e-prints* (May 2018)
44. Tsuzuku, Y., Sato, I., Sugiyama, M.: Lipschitz-margin training: Scalable certification of perturbation invariance for deep neural networks. *NeurIPS* (2018)
45. Uesato, J., O’Donoghue, B., van den Oord, A., Kohli, P.: Adversarial risk and the dangers of evaluating against weak attacks. *CoRR* **abs/1802.05666** (2018), <http://arxiv.org/abs/1802.05666>
46. Verma, V., Lamb, A., Beckham, C., Najafi, A., Mitliagkas, I., Lopez-Paz, D., Bengio, Y.: Manifold mixup: Better representations by interpolating hidden states. In: Chaudhuri, K., Salakhutdinov, R. (eds.) *Proceedings of the 36th International Conference on Machine Learning*. *Proceedings of Machine Learning Research*,

- vol. 97, pp. 6438–6447. PMLR, Long Beach, California, USA (09–15 Jun 2019), <http://proceedings.mlr.press/v97/verma19a.html>
47. Xiao, C., Zhu, J.Y., Li, B., He, W., Liu, M., Song, D.: Spatially transformed adversarial examples. ICLR (2018)
 48. Xie, C., Wu, Y., van der Maaten, L., Yuille, A.L., He, K.: Feature denoising for improving adversarial robustness. CoRR **abs/1812.03411** (2018), <http://arxiv.org/abs/1812.03411>
 49. Xu, K., Liu, S., Zhao, P., Chen, P.Y., Zhang, H., Fan, Q., Erdogmus, D., Wang, Y., Lin, X.: Structured adversarial attack: Towards general implementation and better interpretability. ICLR (2019)
 50. Xu, M., Yu Zhang, J., Ni, B., Li, T., Wang, C., Tian, Q., Zhang, W.: Adversarial domain adaptation with domain mixup. ArXiv **abs/1912.01805** (2019)
 51. Yuan, X., He, P., Zhu, Q., Bhat, R.R., Li, X.: Adversarial examples: Attacks and defenses for deep learning. CoRR **abs/1712.07107** (2017), <http://arxiv.org/abs/1712.07107>
 52. Zhang, C., Hsieh, M.H., Tao, D.: Generalization bounds for vicinal risk minimization principle. arXiv preprint arXiv:1811.04351 (2018)
 53. Zhang, D., Tianyuan, Z., Lu, Y., Zhu, Z., Dong, B.: You only propagate once: Painless adversarial training using maximal principle (05 2019)
 54. Zhang, D., Zhang, T., Lu, Y., Zhu, Z., Dong, B.: You only propagate once: Accelerating adversarial training via maximal principle. arXiv preprint arXiv:1905.00877 (2019)
 55. Zhang, H., Wang, J.: Defense against adversarial attacks using feature scattering-based adversarial training. In: NeurIPS (2019)
 56. Zhang, H., Yu, Y., Jiao, J., Xing, E.P., Ghaoui, L.E., Jordan, M.I.: Theoretically principled trade-off between robustness and accuracy. CoRR **abs/1901.08573** (2019), <http://arxiv.org/abs/1901.08573>
 57. Zhang, H., Cissé, M., Dauphin, Y.N., Lopez-Paz, D.: mixup: Beyond empirical risk minimization. CoRR **abs/1710.09412** (2017), <http://arxiv.org/abs/1710.09412>
 58. Zhao, S., Song, J., Ermon, S.: Infovae: Information maximizing variational autoencoders. CoRR **abs/1706.02262** (2017), <http://arxiv.org/abs/1706.02262>